HYDROGEN, FUEL CELL & ENERGY STORAGE

Analysis and Simulation of the Effect of Combining Load Frequency Control and Automatic Voltage Regulation in Hydrothermal Power System

Majid Moazzami[a,b] | Farhad Faghani[a,c] | Majid Dehghani[a,b,*]
Ghazanfar Shahgholian[a,b] | Mohamadamin Honarvar[a,c] | S. Mohammadali Zanjani[a,b]

[a] Department of Electrical Engineering, Na. C., Islamic Azad University, Najafabad, Iran
[b] Smart Microgrid Research Center, Na. C., Islamic Azad University, Najafabad, Iran
[c] Digital Processing and Machine Vision Research Center, Na. C., Islamic Azad University, Najafabad, Iran
[*] Corresponding author, Email: dehghani@pel.iaun.ac.ir

Article Information

Article Type
Research Article

Article History
Received: *15 Sep 2025*
Revised: *17 Oct 2025*
Accepted: *11 Dec 2025*
Published Online: *05 Jan 2026*

Keywords
Combined control
Frequency control
Hydro unit
Thermal unit
Voltage regulator

Abstract

In modern power systems, load dynamics are always dynamic and constantly changing. To maintain the balance between generation and consumption demand during load fluctuations, power systems must operate intelligently and flexibly. Given the lack of sufficient conventional energy sources, it is essential to combine conventional energy sources with renewable energy sources to balance production-consumption. The integration of renewable power production units with intermittent character will cause the uncertainty of active power generation and the mismatch among the generated energy and the required load causes oscillations in the voltage and frequency of the network. Using the load frequency controller (LFC) to adjust the frequency and the automatic voltage regulator (AVR) to control voltage – through the coordinated management of active and reactive power – is crucial for enhancing power-system stability, especially in the face of sudden changes in energy demand. In this study, the combined LFC-AVR model is considered for a single-area energy grid, which includes a thermal unit and a hydro plant. Synchronous generators with LFC and AVR are important in providing high-quality and uninterrupted electrical power to the network. The primary purpose of investigation and analysis is to show the influence of coupling AVR and LFC loop simultaneously to regulate voltage and frequency. To improve the system response, an integral controller is used in the LFC loop and a proportional-integral (PI) regulator is employed in the AVR loop. The analysis and simulation results show the reduction of frequency and voltage oscillation due to disturbance in the power system.

Cite this article: Moazzami, M., Faghani, F., Dehghani, M., Shahgholian, G., Honarvar, M., Zanjani, M. (2026). Analysis and Simulation of the Effect of Combining Load Frequency Control and Automatic Voltage Regulation in Hydrothermal Power System. DOI: 10.22104/hfe.2025.7649.1366

 Publisher: Iranian Research Organization for Science and Technology (IROST)
DOI: 10.22104/hfe.2025.7649.1366

1 Introduction

The growth in the need for electrical power, along with the reduction of reserves of non-renewable power production units such as coal and diesel, and the production of electrical power from non-renewable sources have caused environmental pollution. The consumption load is changing during the day and night; therefore, energy storage balances the generation and consumption of the power market and reduces the uncertainty of the supply side. Power protection is one of the primary aspects of the expansion and application of microgrids. By being located near loads, microgrids can provide power without loss. Nowadays, many efforts are made to find non-polluting and stable sources due to the lack of transmission systems and to fulfill the request of consumer goods. The performance of the power grid is affected by sudden changes in consumption load and variable power production sources such as photovoltaic panels, solar thermal panels and fuel cells. The employement of renewable power production units causes the diversity and uncertainty of active power production in the power system. This concern has advanced after the growth of renewable power production units and will have a great impact on the active protection of the microgrid, in other words, on the capability of the power grid to conserve the synchronicity of the system when a disturbance occurs [1–14].

1.1 Statement of the problem

A power system consists of connecting many facilities that are connected to each other by means of lines, and are exchanging power with nearby power plants. Power imbalance between production and consumer loads causes frequency and voltage deviation, which may even lead to shutdown. The energy grid is divided into a variety of dispersed generation units to supply power in order to respond to accidental shifts in consumption load. The complexity and scale of interconnected power systems have increased dramatically. The simultaneous requlation of voltage and frequency in the energy network is one of the central issues. The importance of voltage and frequency controllers has increased with the expansion of related parts in the operation of modern energy networks to deliver energy in system operation with a high level of reliability. Voltage fluctuations and load frequency fluctuations depend on reactive power and active power, respectively. Therefore, the production units have two control loops, AVR and LFC, which are responsible for the frequency regulator and the terminal voltage regulator, respectively. The load frequency regulation loop is used to optimize the frequency and energy variations of the connection line between the areas. The automatic voltage regulator holds the terminal voltage of the synchronous generator at the nominal grade using excitation voltage control. It is possible for loads to appear randomly and variable in different areas of the corresponding energy grid, which causes deviation of the grid frequency and energy of the connecting line from the nominal values. In general, the two main goals of control systems in a connected energy grid, while maintaining the energy quality at the required level, are: the instantaneous matching of production with the system load along with system frequency regulation, and power transmission in the connection line according to the programmed weights. Figure 1 shows the structure of a synchronous machine with two regulation structures [15–28].

1.2 Literature surveys

The energy grid unit's stability is affected by the deviation in the voltage levels, so AVR is employed to follow the reference voltage. The dynamic changes of the load affect the frequency deviation, and therefore, in order to prevent the spread of frequency fluctuations to the energy grid, LFC is used. For the correct function of both AVR and LFC systems, a controller is required, whose parameters must be selected for the best controller performance. So far, various studies have shown the effect of these two controllers in the power system [29–37].

The durable design of hybrid designs of two AVR and LFC controllers was achieved in a multi-zone energy grid using a non-linear limit accepting algorithm (NLTA) [38]. This method reveals the improvement of the energy grids designed according to the separate approaches of using these two controllers. Moreover, the development of the use of NLTA in large power systems is shown. The incorporated regulation of LFC and AVR in a three-zone power system including water, gas, and geothermal units is presented in [39], where nonlinear constraints are considered for the energy network. In this study, the effects of different power storage units on the hybrid controller were investigated.

The coordinated performance of the FACTS device controller and the power system stabilizer in a two-zone power system (each zone includes three production units) equipped with two LFC and AVR controllers has been analyzed and simulated in [40]. The secondary controller is used in both control loops and lightning search algorithm is used to optimize the controller parameters. The simulation results show the effectiveness of combined PSS and interline power flow controller control compared to their individual use.

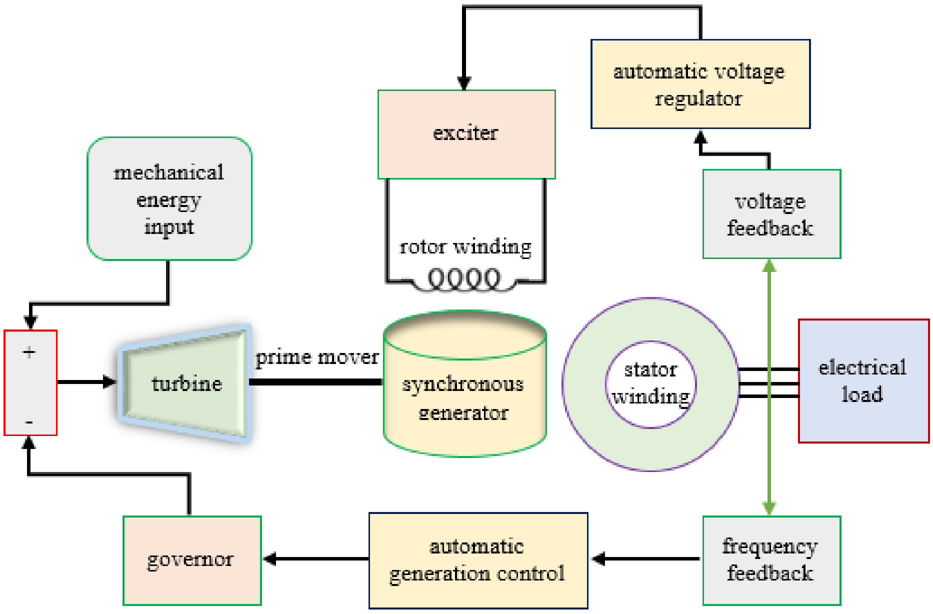

Fig. 1. Synchronous generator with two controllers.

The large penetration of renewable energy into the power system increases the communication load, which may have a negative impact on the system control performance. In order to reduce the network congestion caused by bandwidth limitations, an improved scheme with integral event trigger is presented in [41]. The challenges associated with automatic voltage regulation and load frequency control in the power system are investigated. The proposed method includes two time delays and external disturbances, and the historical output of the system is used to select the data to the controller.

The function of a corresponding energy grid depends on the performance of the controllers, and therefore regulating the terminal voltage and frequency simultaneously requires an intelligent control strategy. In [42], the control method based on the PID regulator in a multi-zone connected energy network has been investigated, where two control loops are considered in each zone. Controllers are designed with computational algorithms inspired by nature. The changes in the parameters of the behavior of the regulators in a three-zone energy network are shown.

LFC and AVR control loops in interconnected power grids are essential for effective frequency and voltage regulation in the power system to maintain a stable power supply, which the integration of renewable energy sources poses challenges for this type of control loop. The impact of using different operating strategies on the control loops in a two-zone power system with doubly-fed induction generators is investigated in [43], where the strategies are based on frequency-related pricing under access-based tariff. The faster operation of the proposed method compared to traditional methods helps to maintain frequency and voltage during load disturbances.

To support the performance and security of production systems, AVR and LFC control loops are used in the main power networks, which also improves stability. For this purpose, a numerical solution based on heuristics for multi-objective optimization of controller gains in LFC-AVR scheme is presented in [44]. The proposed method has been used in a two-zone power system to ensure stable generator-bus frequency and voltage regulation under dynamic disturbances.

1.3 Contribution and structure

To achieve reliability in power system operation, the optimal operating level in the electrical energy system must be maintained. In other words, the system must operate at the nominal frequency. Load frequency control and excitation system voltage regulation are usually non-interactive and independently modeled and analyzed. In this study, two simultaneous control loops are considered, and the performance of the single-zone energy system is simulated for load shifts. The modes of the network have been determined using differential equations in the state space and the simulation results have been analyzed. Therefore, the research primary objectives are:

- Development of multi-source single-zone power

system equipped with LFC control system with the addition of AVR control system
- Comparison of dynamic responses to changes in system parameters and load changes
- Expressing the system equations in state-space form and evaluating system performance through eigenvalue analysis – Showing the necessity of combining two control loops

The remaining parts of this study are as follows: The studied power system structure is defined in section 2, whose equations are represented in the form of state space. In section 3, the simulation results for load changes are shown, and then the results are discussed using system modes. Ultimately, the conclusion is stated in section 4.

2 Dynamic Model of Power System under Study

The studied single-area energy system consists of a heater part and a water part, which is used to adjust the frequency of the LFC loop and to adjust the voltage of the AVR loop. The change of active power in the production line in grid hydropower plants impacts the frequency of the all energy system. The performance of a hydropower plant depends on the frequency, and its regulation is necessary to provide quality power. The model of production units can be displayed using first-order differential equations [45–48].

2.1 Load frequency regulation

The load demand in the energy system is constantly variable, which leads to power imbalance. Power imbalance in the load or generation source due to changes in renewable power production units causes frequency variation in the energy network. The load frequency regulation loop is used to provide a trade-off among active energy and frequency management. The LFC system is an independent subsystem in each area [49, 50].

Figure 2 illustrates the first level of frequency regulation, representing a single-area energy network with two sources. The characteristics of the transfer processes constituting the LFC scheme representative are given in Table 1 along with the definition of the parameters. Due to the importance of balancing the generation and demand of active power, secondary control (load frequency control) has an important role in power system control. Due to the mismatch between the generation and demand of the load, the performance of the power system will be disrupted due to continuous changes in frequency, inter-area power, and voltage. In primary control, frequency changes are responded by the turbine speed governor. In the event of abnormal conditions, the secondary control loop will be activated, and in this case, the available stored energy is used to restore the system frequency. For large disturbances that result in a significant imbalance between generation and load demand, the tertiary control loop is employed to limit frequency deviations and stabilize the system [51–53].

The transfer function of the rotating system and the load is represented by a first-order transfer function as follows, whose output is considered as the first state variable x_1. This state variable represents the changes in the output frequency of the power system.

$$G_{\mathrm{PS}}(s) = \frac{K_{\mathrm{PS}}}{T_{\mathrm{PS}}s + 1}\,. \tag{1}$$

The transfer functions shown in the block diagram of a hydro turbine power plant are:

$$G_{\mathrm{HT}}(s) = \frac{1 + T_W s}{1 - 0.5T_W s}\,, \tag{2}$$

$$G_{\mathrm{TD}}(s) = \frac{T_{\mathrm{RS}} + 1}{T_{\mathrm{RH}}s + 1}\,, \tag{3}$$

$$G_{\mathrm{HG}}(s) = \frac{K_{\mathrm{GH}}}{T_{\mathrm{GH}}s + 1}\,. \tag{4}$$

The state variables x_2, x_3, and x_4 represent the output of each of the blocks defined above, respectively. The transfer functions representing the block diagram of a steam turbine power plant are defined as follows:

$$G_{\mathrm{TT}}(s) = \frac{K_{\mathrm{TT}}}{T_{\mathrm{TT}}s + 1}\,, \tag{5}$$

$$G_{\mathrm{RH}}(s) = \frac{K_R T_R s + 1}{T_R s + 1}\,, \tag{6}$$

$$G_{\mathrm{TG}}(s) = \frac{K_{\mathrm{GT}}}{T_{\mathrm{GT}}s + 1}\,. \tag{7}$$

In this case, the state variables x_5, x_6, and x_7 represent the outputs of the considered blocks, respectively. In the LFC loop, an integrator controller is used, which has the following transfer function. Moreover, its output variable is considered as the x_8 state variable:

$$G_{\mathrm{CF}}(s) = \frac{K_{\mathrm{IF}}}{s}\,. \tag{8}$$

2.2 Automatic voltage control

The AVR control loop has a faster reaction than the LFC control part and as a result, the LFC system will have little impact on the AVR loop, but the effect of AVR system on LFC loop is considerable. The voltage protection of the synchronous generator is the responsibility of the automatic voltage regulator.

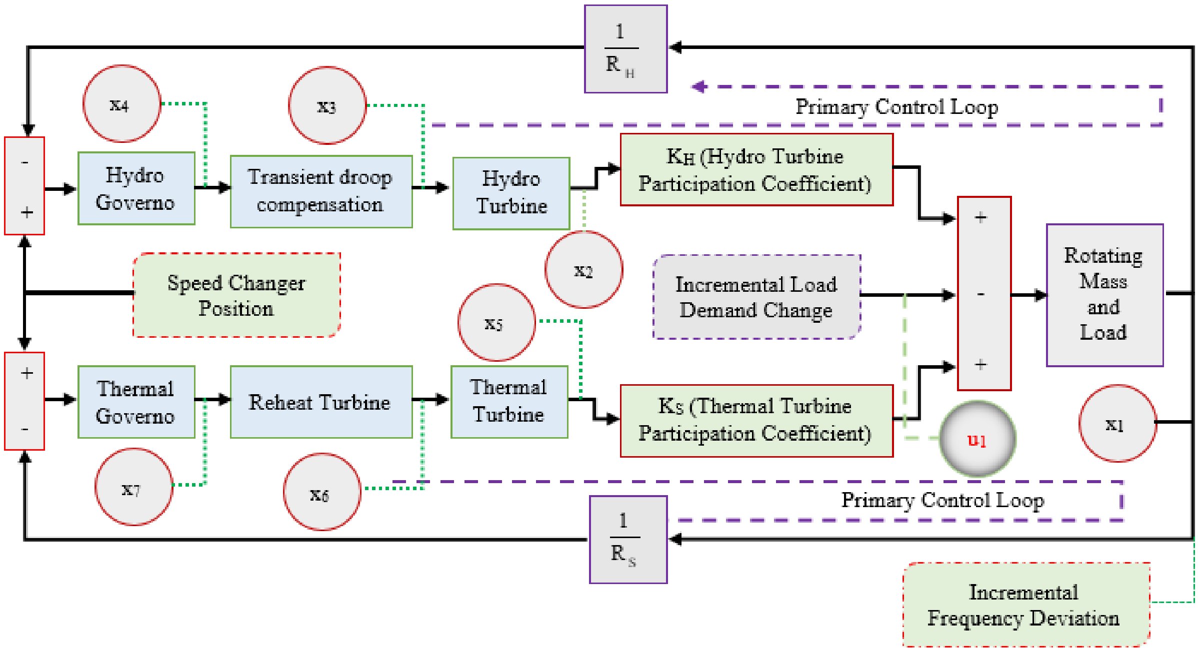

Fig. 2. Load frequency control model for multi-source single-area power system based transfer function.

Table 1. Characteristics of load frequency control subsystems.

Sub-system		Parameters	Parameter description
Hydro power plant	Penstock hydro turbine	T_W	Water starting time
	Transient droop compensation	T_{RS}	Hydro turbine speed governor reset time
		T_{RH}	Time-constant of the transient droop
	Hydro governor	K_{GH}	Governor gain
		T_{GH}	Governor time constant
Thermal power plant	Thermal turbine	K_{TT}	Turbine gain
		T_{TT}	Turbine time constant
	Reheat turbine	T_R	Reheat time constant
		K_R	Reheat constant
	Thermal governor	K_{GT}	Governor gain
		T_{GT}	Governor time constant
Power system	Rotating mass and load	T_{PS}	Time constant
		K_{PS}	Gain
Controller	Speed changer position	K_{IF}	Controller integral gain

Adjusting the generator terminal voltage maintains power quality. The generator voltage is regulated using the controller based on the reference signal by controlling the field winding of machine. Frequency change affects the generator terminal voltage but is neutralized by the fast operation of the AVR loop, while the generator terminal voltage can control the system frequency by affecting the active power. The time constants of the voltage control loop are much shorter than the time constants of the frequency control loop [54–57].

The block diagram of AVR system consists of blocks related to generator excitation field, excitation unit (synchronous generator field changer), sensor unit (terminal voltage measurement) and amplifier unit (error signal amplification) [58,59]. The synchronous machine relationships are related to the terminal voltage, the active power balance and the oxide system, which are manifested by the linearization of these relationships of the synchronous car with six K_1 to K_6.

Figure 3 shows the AVR system with K coefficients consisting of four first-order subsystem structures, the specifications of the subsystems are given in Table 2 [60, 61]. The output of each subsystem is defined as a state variable. The coefficients of the participation of the two production units with K_H and K_S are shown, which are related to the water unit and the steam unit, respectively.

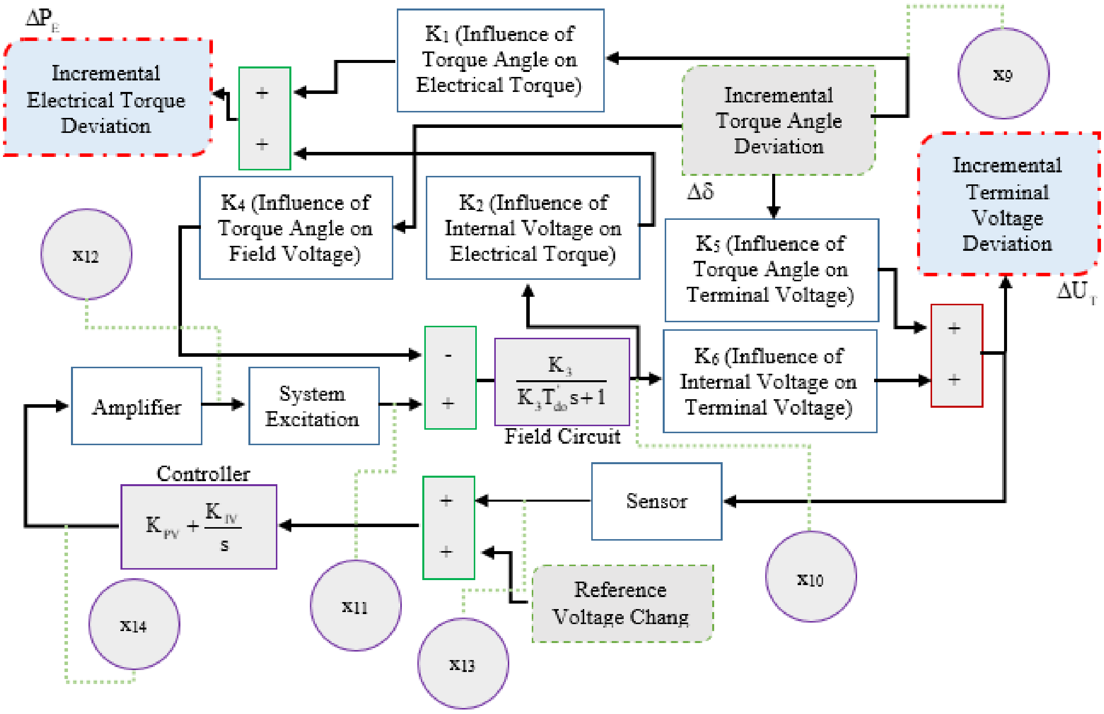

Fig. 3. Automatic voltage controller model based on transfer functions.

Table 2. Characteristics of automatic voltage regulator subsystems

Sub-system	Gain and time constant	Range of parameter changes
Generator field	K_3	0.7-1
	T_{do}	1.5-10
System excition	K_E	1-10
	T_E	0.5-1
Amplifier	K_A	10-40
	T_A	0.02-0.1
Voltage sensor	K_S	1
	T_S	0.001-0.06
Controller	Proportional gain	K_P
	Integral gain	K_I

The block diagram of the AVR loop is shown with four transfer functions, whose outputs represent the state variables x_{10}, x_{11}, x_{12}, and x_{13}, respectively.

$$G_F(s) = \frac{K_3}{K_3 T_{\text{do}} s + 1}\,, \tag{9}$$

$$G_E(s) = \frac{K_{\text{PS}}}{T_E s + 1}\,, \tag{10}$$

$$G_A(s) = \frac{K_A}{T_A s + 1}\,, \tag{11}$$

$$G_S(s) = \frac{K_S}{T_S s + 1}\,. \tag{12}$$

A proportional-integral controller is used for the AVR loop, with the state variable x_{14} being considered for the integrator part.

$$G_C(s) = K_P + \frac{K_1}{s}\,. \tag{13}$$

2.3 System equations in state space

The combination of two LFC and AVR systems along with two generating units forming one area is shown in Figure 4. The studied energy network model can be assumed a linear time varing dynamic system whose equations are expressed in the state space as follows [62]:

$$\frac{d\mathbf{X}}{dt} = \mathsf{A}\mathbf{X} + \mathsf{B}\mathbf{U} + \Gamma\mathbf{D}\,, \tag{14}$$

$$\mathbf{Y} = \mathsf{C}\mathbf{X}\,, \tag{15}$$

where **X**, **U**, and **D** are the vectors of state variables, independent input, and disturbance input, respectively. The **Y** vector shows the output variables (case of study). Likewise, A, B, and C are the system, control, and output matrices, respectively, and Γ is the disturbance matrix. State variables include three categories of variables related to water unit, steam unit, and AVR. Output variables are frequency changes and output mechanical energy of generation systems. A total of 14 differential equations are extracted to represent the energy network representative in the state-space [63].

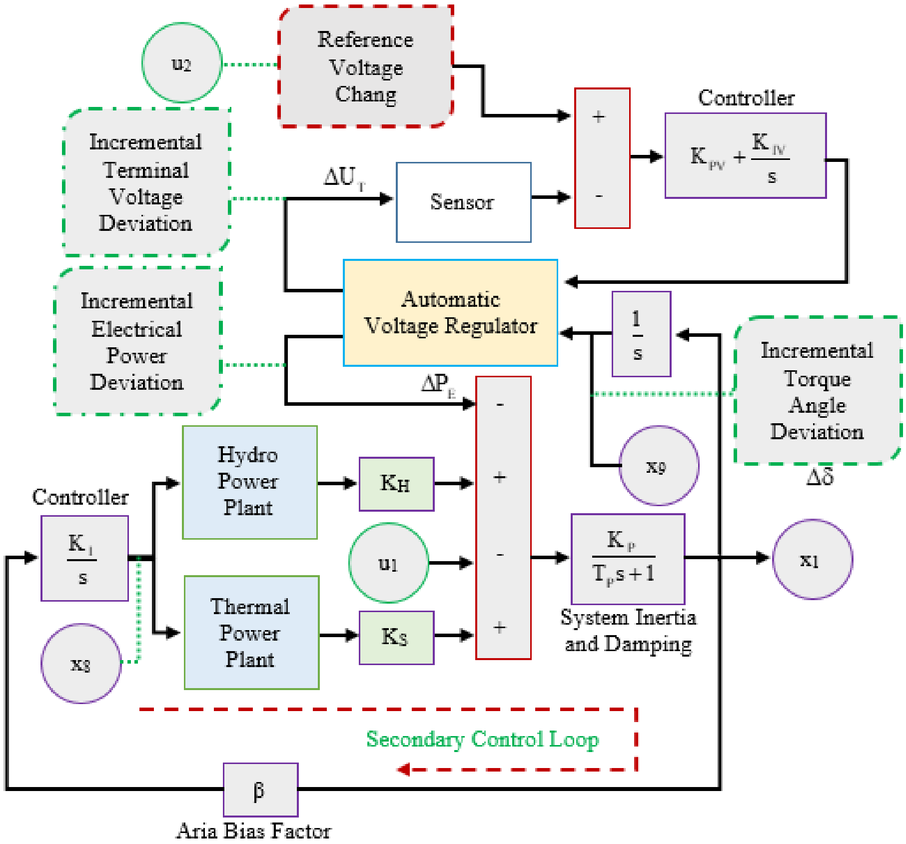

Fig. 4. Combined LFC-AVR model of multi-source single-area power system.

$$\frac{dx_1}{dt} = -\frac{1}{T_{\text{PS}}}x_1 + \frac{K_H K_{\text{PS}}}{T_{\text{PS}}}x_2 + \frac{K_S K\text{PS}}{T_{\text{PS}}}x_5 - \frac{K_{\text{PS}}}{T_{\text{PS}}}u_1 - \frac{K_{\text{PS}}}{T_{\text{PS}}}(K_1 x_9 + K_2 x_{10}), \quad (16)$$

$$\frac{dx_2}{dt} = -\frac{2}{T_W}x_2 + \frac{2}{T_W}x_3 - 2\frac{dx_3}{dt} \quad (17)$$

$$\frac{dx_3}{dt} = -\frac{1}{T_{\text{RH}}}x_3 + \frac{1}{T_{\text{RH}}}x_4 + \frac{T_{\text{RS}}}{T_{\text{RH}}}\frac{dx_4}{dt}, \quad (18)$$

$$\frac{dx_4}{dt} = -\frac{1}{T_{\text{GH}}}x_4 + \frac{K_{\text{GH}}}{T_{\text{GH}}}x_8 - \frac{K_{\text{GH}}}{T_{\text{GH}}}\frac{1}{R_H}x_1, \quad (19)$$

$$\frac{dx_5}{dt} = -\frac{1}{T_{\text{TT}}}x_5 + \frac{K_{\text{TT}}}{T_{\text{TT}}}x_6, \quad (20)$$

$$\frac{dx_6}{dt} = -\frac{1}{T_R}x_6 + \frac{1}{T_R}x_7 + K_R\frac{dx_7}{dt}, \quad (21)$$

$$\frac{dx_7}{dt} = -\frac{1}{T_{\text{GS}}}x_7 + \frac{K_{\text{GS}}}{T_{\text{GS}}}x_8 - \frac{K_{\text{GS}}}{T_{\text{GS}}}\frac{1}{R_S}x_1, \quad (22)$$

$$\frac{dx_8}{dt} = K_1 \beta x_1, \quad (23)$$

$$\frac{dx_9}{dt} = 2\pi x_1, \quad (24)$$

$$\frac{dx_{10}}{dt} = -\frac{1}{K_3 T_{\text{do}}}x_{10} + \frac{1}{T_{\text{do}}}(x_{11} - K_4 x_9), \quad (25)$$

$$\frac{dx_{11}}{dt} = -\frac{1}{T_E}x_{11} + \frac{K_E}{T_E}x_{12}, \quad (26)$$

$$\frac{dx_{12}}{dt} = \frac{-1}{T_A}x_{12} + \frac{K_A}{T_A}(x_4 - K_{\text{PV}}x_{13} + K_{\text{PV}}u_2), \quad (27)$$

$$\frac{dx_{13}}{dt} = -\frac{1}{T_S}x_{13} + \frac{K_S}{T_S}(K_5 x_9 + K_6 x_{10}), \quad (28)$$

$$\frac{dx_{14}}{dt} = K_{\text{IV}}(u_2 - x_{13}). \quad (29)$$

3 Simulation Results

Reliable power generation and load supply are two main objectives in the energy network to keeo voltage and frequency stability while observing permissible limits. The frequency, voltage and power exchanged between interconnected areas in the power system deviate from their nominal values due to changes in power demand, which can be reduced by controlling the governor in the load frequency regulation system and by exciting the generator in the automatic voltage regulator system [64]. In addition to modeling using state space, the power system under investigation has also been implemented in the MATLAB/Simulink space to verify the simulation results as shown in Figure 5.

The power system under study has two inputs. In this section, the simulation results of three different scenarios are shown. Since a linearized system model is used, the system modes do not depend on the location of the input.

The parameters related to the hydro generation unit are: $K_{\rm GH} = 1$, $R_H = 0.05$, $T_{\rm GH} = 0.2$, $T_W = 1$, $T_{\rm RS} = 5$, $T_{\rm RH} = 0.38T_{\rm RS}/R_H$ and the parameters related to the steam generation unit are: $R_S = 0.05$, $K_{\rm TT} = 1$, $T_T = 0.3$, $K_R = 0.3$, $T_R = 7$, $K_{\rm GS} = 1$ and $T_{\rm GS} = 0.2$. The control system parameters are: $K_{\rm IF} = 0.5$, $K_{\rm PV} = 0.2$, $K_{\rm IV} = 0.1$. Also, the K constants related to the synchronous generator are: $K_1 = 0.5794$, $K_2 = 1.0976$, $K_3 = 0.6250$, $K_4 = 0.8232$, $K_5 = -0.1458$ and $K_6 = 0.6860$.

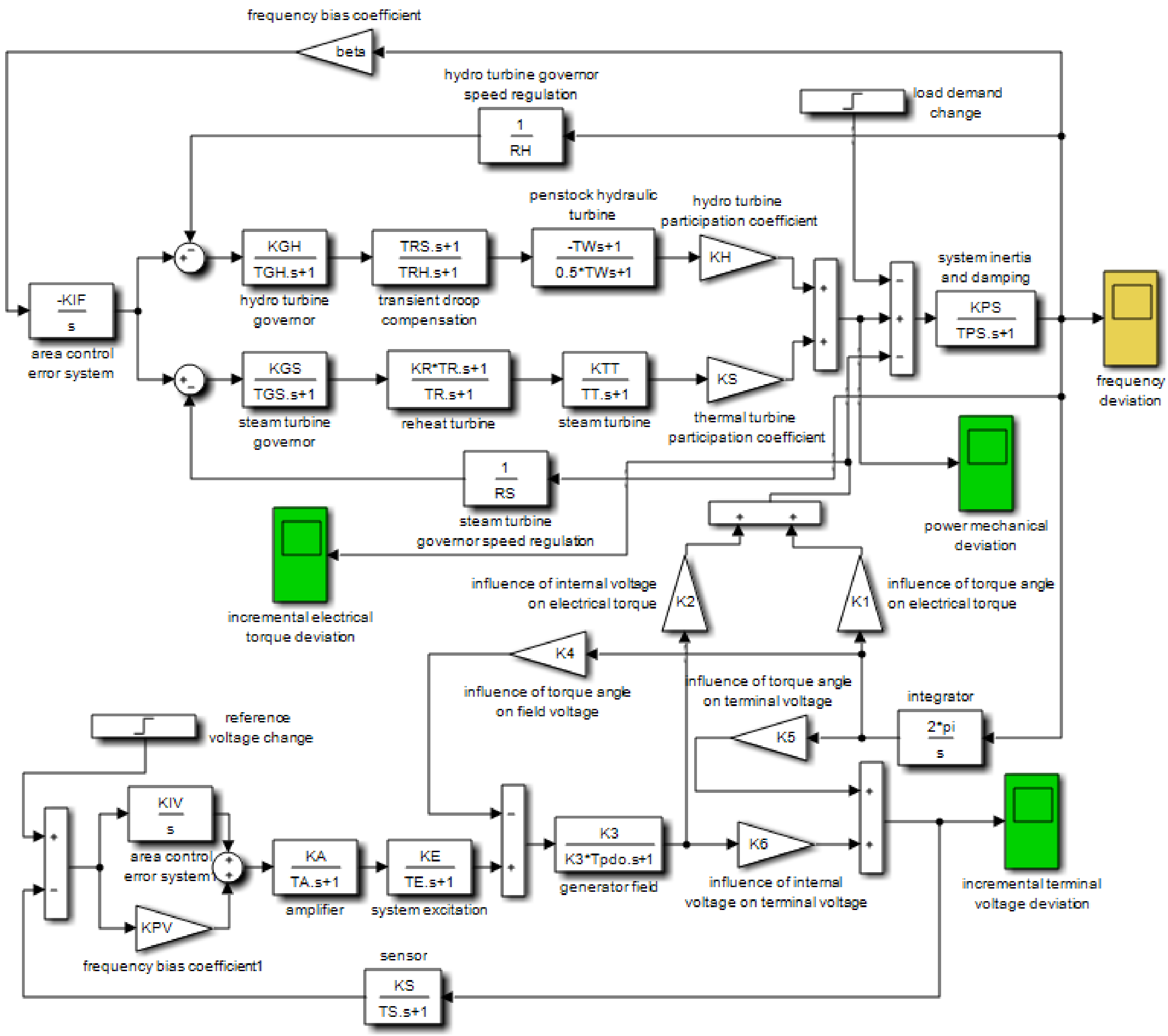

Fig. 5. Implementation of the studied power system model in MATLAB Simulink.

3.1 Scenario A

In this case, only the LFC control loop is considered. The order of the system is 8, and the eigenvalues of the system matrix are: -6.2397, -5.0000, -2.8284, -0.4923, -0.0427, -0.0074 and $-0.4960 \pm j1.0642$. The system has one oscillation mode whose damping coefficient is 0.4224. The system frequency changes and mechanical power changes of the two generating units for step load changes are shown in Figures 6 and 7. In this case, only the LFC control loop is considered, and the AVR control loop is out of the circuit.

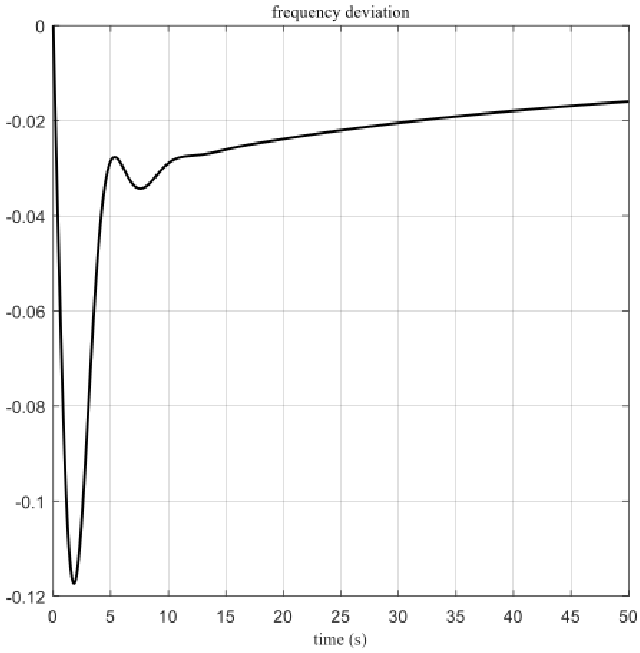

Fig. 6. System frequency changes per change with only LFC control loop.

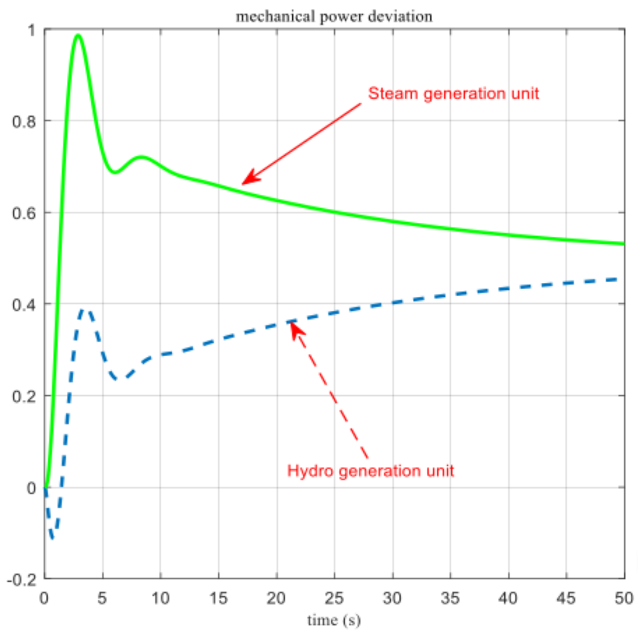

Fig. 7. Mechanical power changes of two generating units for changes with only one LFC control loop.

3.2 Scenario B

In this case, both the load changes and the reference voltage changes are considered as steps. In this case, both the load and the voltage reference change in a stepwise manner simultaneously. The system under study is of order 14, so the eigenvalues of the system matrix are: $-20.0326 \pm j0.7933$, -6.2312, -5.0000, -2.8352, -1.3041, -0.8376, $-0.3644 \pm j1.2325$, -0.1054, -0.0246, 0.0000 and $-0.1716 \pm j0.4590$. The system has three oscillation modes whose damping coefficients are 0.9992, 0.2835 and 0.3502.

As can be seen, all modes are in the left-axis imaginary system, so the system will be stable with the designed controllers. The simulation results, including system frequency changes, generator terminal voltage changes, and electric torque changes when both control loops exist in the power system, are shown in Figure 8. Also, the mechanical power changes of two generating units for step changes in load when both control loops are present in the power system are shown in Figure 9. As can be seen, the system response is stable in this case as well.

3.3 Scenario C

In this section, the load changes are considered in multi-steps as shown in Figure 10. The simulation results are shown in Figure 11. As can be seen, after each step change, the frequency changes have reached a stable state, and finally, the changes have tended to zero due to the presence of controllers.

4 Conclusion

Frequency and voltage are two key aspects of a power system, and their control is very important. The stability of the energy network because of load shifts depends on the control of terminal voltage and frequency of the grid. The frequency is related to the active energy output, and it needs to be managed and maintained fixed under different system functionalities. A change in the consumption load or a disturbance in the energy grid affects the demands of reactive and active energy, which will affect the normal operation of the power system. A coupling of load frequency regulation and an automatic voltage regulator system is employed to maintain frequency and terminal voltage in nominal values. In this study, the behavior of a multi-source single-area energy grid is considered to investigate the effect of frequency and voltage control loops. The simulation results are analyzed based on system modes. The simulation results are shown in three scenarios including only LFC control loop, two control loops with step load changes and two control loops with multi-step load changes in the time domain. This method can be extended to multi-zone power systems.

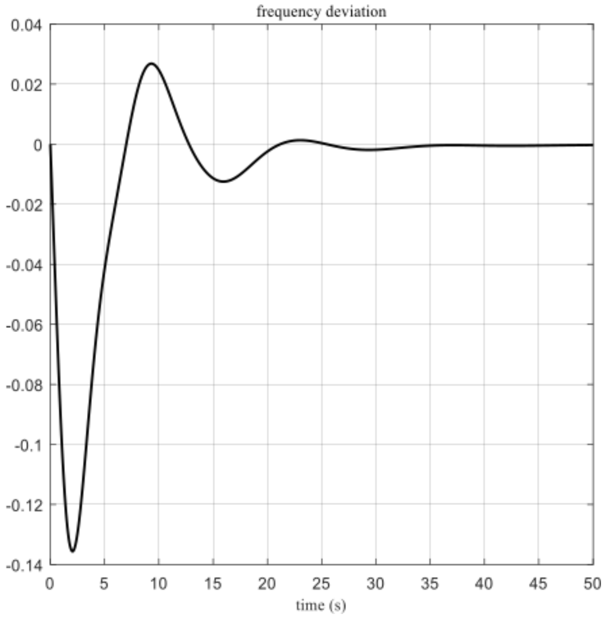

(a) System frequency changes

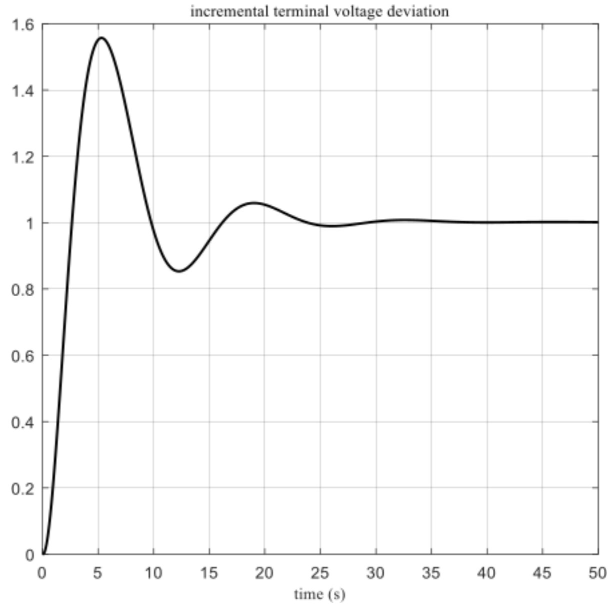

(b) Terminal voltage changes

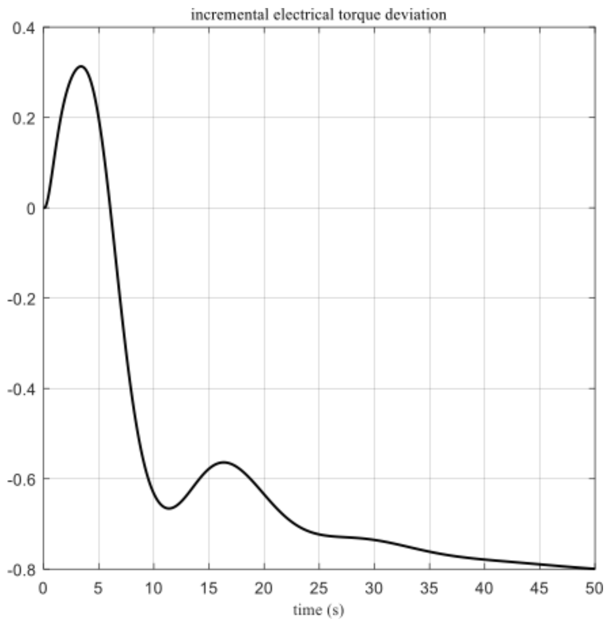

(c) Electrical torque changes

Fig. 8. Simulation results for step load changes with both control loops

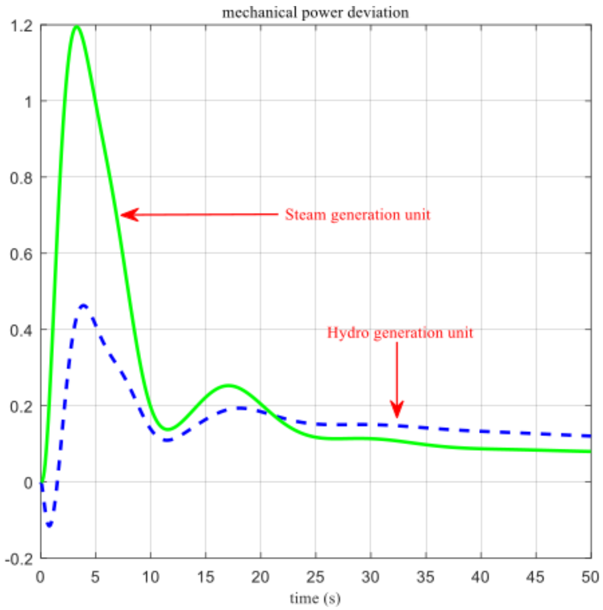

Fig. 9. Mechanical power changes of two generation units with two control loops.

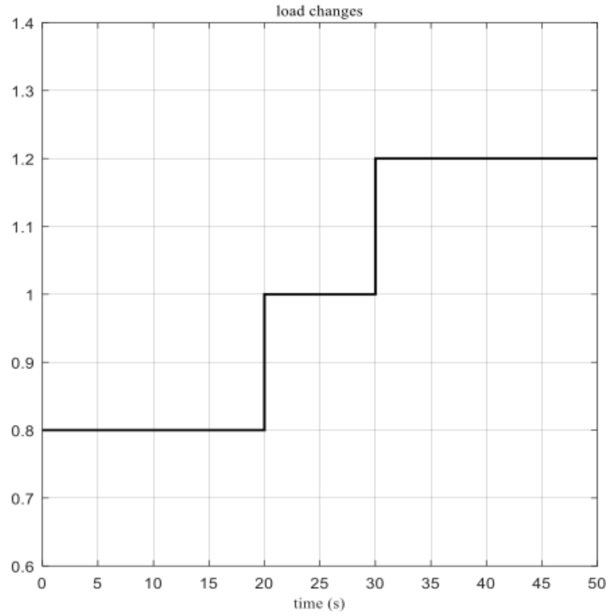

Fig. 10. Stepped load changes in a power system with two control loops.

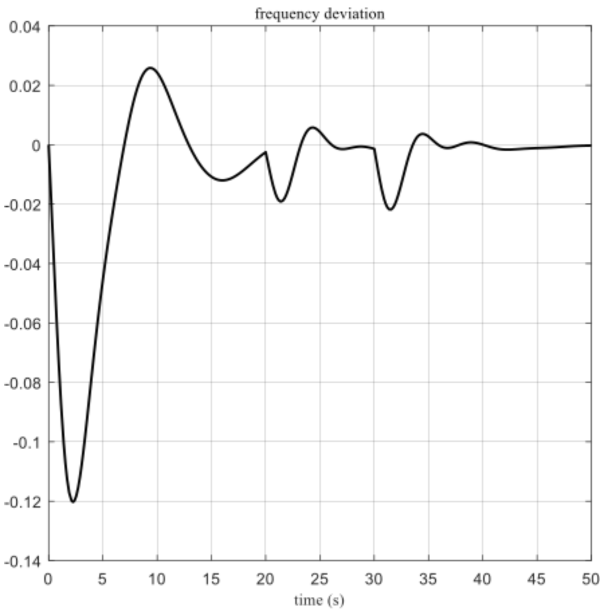

(a) System frequency changes

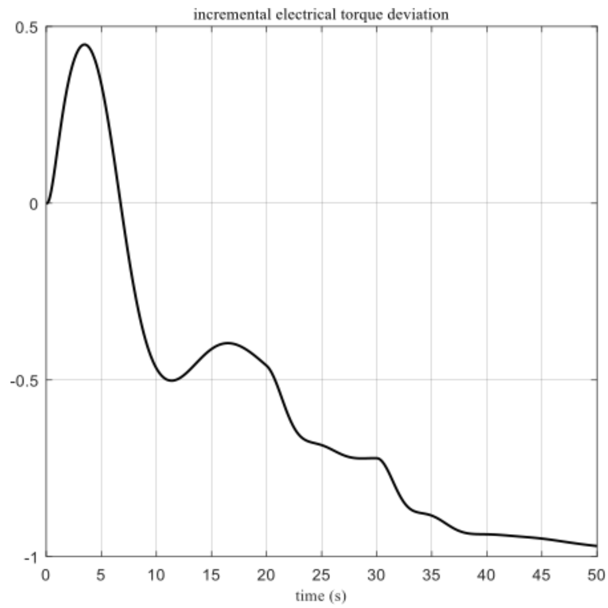

(b) Terminal voltage changes

Fig. 11. System response in multi-steps changes in load

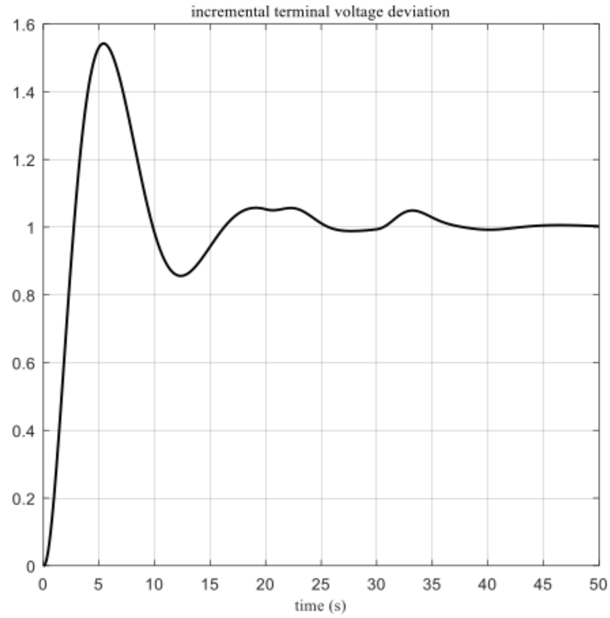

(c) Electrical torque changes

Fig. 11. (*Continued*)

Acknowledgment

The authors express their sincere gratitude to the reviewers for their insightful comments. They also extend their appreciation to the journal's esteemed colleagues for their diligent efforts.

References

[1] Tayab UB, Roslan MAB, Hwai LJ, Kashif M. A review of droop control techniques for microgrid. Renewable and Sustainable Energy Reviews. 2017;76:717-27.

[2] Fathollahi A, Andresen B. Adaptive fixed-time control strategy of generator excitation and thyristor-controlled series capacitor in multi-machine energy systems. IEEE Access. 2024.

[3] Shahgholian G, Fathollahi A. Advancing load frequency control in multi-resource energy systems through superconducting magnetic energy storage. AppliedMath. 2025;5(1):1.

[4] Forouzandehmehr N, Han Z, Zheng R. Stochastic dynamic game between hydropower plant and thermal power plant in smart grid networks. IEEE Systems Journal. 2014;10(1):88-96.

[5] Siti M, Mbungu N, Tungadio D, Banza B, Ngoma L. Application of load frequency control method to a multi-microgrid with energy storage system. Journal of Energy Storage. 2022;52:104629.

[6] Veronica AJ, Kumar NS. Control strategies for frequency regulation in microgrids: A review. Wind Engineering. 2021;45(1):107-22.

[7] Coban HH, Rehman A, Mousa M. Load frequency control of microgrid system by battery and pumped-hydro energy storage. Water. 2022;14(11):1818.

[8] Shahgholian G, Izadpanahi N. Improving the performance of wind turbine equipped with DFIG using STATCOM based on input-output feedback linearization controller. Energy Equipment and Systems. 2016.

[9] Fathollahi A, Gheisarnejad M, Andresen B, Farsizadeh H, Khooban MH. Robust artificial intelligence controller for stabilization of full-bridge converters feeding constant power loads. IEEE Transactions on Circuits and Systems II: Express Briefs. 2023;70(9):3504-8.

[10] Magdy G, Mohamed EA, Shabib G, Elbaset AA, Mitani Y. Microgrid dynamic security consider-

ing high penetration of renewable energy. Protection and Control of Modern Power Systems. 2018;3(3):1-11.

[11] Gamage D, Wanigasekara C, Ukil A, Swain A. Multi-level consensus based load frequency controller with multi-battery energy storage systems. Electric Power Systems Research. 2025;239:111208.

[12] Patel R, Wanigasekara C, Swain A, Ukil A. Consensus-based Load Frequency Control of a Multi-Area Power System. IEEE Access. 2024.

[13] Alnefaie SA, Alkuhayli A, Al-Shaalan AM. Optimizing Load Frequency Control of Multi-Area Power Renewable and Thermal Systems Using Advanced Proportional–Integral–Derivative Controllers and Catch Fish Algorithm. Fractal and Fractional. 2025;9(6):355.

[14] Shahgholian G, Zanjani SMA. A study of voltage sag in distribution system and evaluation of the effect of wind farm equipped with doubly-fed induction generator. REVUE ROUMAINE DES SCIENCES TECHNIQUES—SÉRIE ÉLECTROTECHNIQUE ET ÉNERGÉTIQUE. 2023;68(3):271-6.

[15] Marjanian A, Solaymani S, Shahgholian G, et al. Designing an emotional intelligent controller for IPFC to improve the transient stability based on energy function. Journal of Electrical Engineering & Technology. 2013;8(3):478-89.

[16] Aghadavoodi E, Shahgholian G. A new practical feed-forward cascade analyze for close loop identification of combustion control loop system through RANFIS and NARX. Applied Thermal Engineering. 2018;133:381-95.

[17] Kazemi-Esfeh N, Baharizadeh M. A decentralized control method based on virtual frequency-voltage frame for accurate active and reactive powers sharing in microgrids. Journal of Intelligent Procedures in Electrical Technology. 2023;14(55):55-66.

[18] Chicco G, Mancarella P. Distributed multi-generation: A comprehensive view. Renewable and sustainable energy reviews. 2009;13(3):535-51.

[19] Fathollahi A, Andresen B. Deep deterministic policy gradient for adaptive power system stabilization and voltage regulation. e-Prime-Advances in Electrical Engineering, Electronics and Energy. 2024;9:100675.

[20] Ullah K, Basit A, Ullah Z, Aslam S, Herodotou H. Automatic generation control strategies in conventional and modern power systems: A comprehensive overview. Energies. 2021;14(9):2376.

[21] Awda Y, Alowaifeer M. Adaptive optimization of virtual synchronous generator based on fuzzy logic control and differential evolution. Ain Shams Engineering Journal. 2024;15(4):102606.

[22] Singh A, Sharma V, Kumar V, Naresh R, Rahi OP. AOA based optimal control of combined AVR-LFC model in wind integrated power system. Wind Engineering. 2023;47(3):515-27.

[23] Kalyan CHNS, Rao GS. Impact of communication time delays on combined LFC and AVR of a multi-area hybrid system with IPFC-RFBs coordinated control strategy. Protection and Control of Modern Power Systems. 2021;6(1):1-20.

[24] Gupta M, Srivastava S, Gupta J. A novel controller for model with combined LFC and AVR loops of single area power system. Journal of The Institution of Engineers (India): Series B. 2016;97(1):21-9.

[25] Kumar M, Hote YV. Graphic RCRA-PIDA tuning based on maximum sensitivity for automatic generation control of thermal and hydro power systems. IET Generation, Transmission & Distribution. 2020;14(26):6427-39.

[26] Elsisi M, Soliman M, Aboelela M, Mansour W. Optimal design of model predictive control with superconducting magnetic energy storage for load frequency control of nonlinear hydrothermal power system using bat inspired algorithm. Journal of Energy Storage. 2017;12:311-8.

[27] Abraham RJ, Das D, Patra A. Automatic generation control of an interconnected hydrothermal power system considering superconducting magnetic energy storage. International Journal of Electrical Power & Energy Systems. 2007;29(8):571-9.

[28] Riahinasab M, Behzadfar N, Movahednejad H. Analysis and Simulation of Load Frequency Control in Power System with Reheater Steam Turbine. power. 2022;10:11.

[29] Peddakapu K, Mohamed M, Srinivasarao P, Arya Y, Leung P, Kishore D. A state-of-the-art review on modern and future developments of AGC/LFC of conventional and renewable energy-based power systems. Renewable Energy Focus. 2022;43:146-71.

[30] Bora Ç, Kerim D, Şeymanur B, Erdinç Ş, Mehmet NF. A novel objective function design and detailed analysis for the AVR-LFC system. Sādhanā. 2023;48(4):229.

[31] Pathak N, Verma A, Bhatti TS. Automatic generation control of thermal power system under varying steam turbine dynamic model parameters based on generation schedules of the plants. The Journal of Engineering. 2016;2016(8):302-14.

[32] Elsaied MM, Abdel Hameed WH, Hasanien HM. Frequency stabilization of a hybrid three-area power system equipped with energy storage units and renewable energy sources. IET Renewable Power Generation. 2022;16(15):3267-86.

[33] Alharbi M, Ragab M, AboRas KM, Kotb H, Dashtdar M, Shouran M, et al. Innovative AVR-LFC design for a multi-area power system using hybrid fractional-order PI and PIDD2 controllers based on dandelion optimizer. Mathematics. 2023;11(6):1387.

[34] Huo Z, Xu C. Multi-event collaborative triggering mechanism based distributed robust fault-tolerant load frequency control for offshore wind power systems. Ocean Engineering. 2025;333:121424.

[35] Guo J. The load frequency control by adaptive high order sliding mode control strategy. IEEE access. 2022;10:25392-9.

[36] Guo J. A novel proportional-derivative sliding mode for load frequency control. IEEE Access. 2024.

[37] Pradana A, Nadarajah M, Feng J, Haque MM. Mitigating Cyberattack Impacts on LFC-AVR Systems with High Renewable Penetration through Redundancy and Adaptive Kalman Filter. In: 2025 7th Global Power, Energy and Communication Conference (GPECOM). IEEE; 2025. p. 839-44.

[38] Nahas N, Abouheaf M, Sharaf A, Gueaieb W. A self-adjusting adaptive AVR-LFC scheme for synchronous generators. IEEE Transactions on Power Systems. 2019;34(6):5073-5.

[39] Dekaraja B, Saikia LC, Ramoji SK, Behera MK, Bhagat SK. Performance analysis of diverse energy storage on combined ALFC and AVR control of Multiarea multiunit system with AC/HVDC interconnection. IFAC-PapersOnLine. 2022;55(1):479-85.

[40] Weldcherkos T, Salau AO, Ashagrie A. Modeling and design of an automatic generation control for hydropower plants using Neuro-Fuzzy controller. Energy Reports. 2021;7:6626-37.

[41] Li Z, Liu J, Li H, Zhang P, Zhang Y. An Integral-event-triggered Scheme for AVR-LFC Optimization Strategy with Guaranteed L_∞-Gain. In: 2023 5th International Conference on Electrical Engineering and Control Technologies (CEECT). IEEE; 2023. p. 240-4.

[42] Rajbongshi R, Saikia LC. Performance of coordinated interline power flow controller and power system stabilizer in combined multiarea restructured ALFC and AVR system. International Transactions on Electrical Energy Systems. 2019;29(5):e2822.

[43] Dholakiya VM, Suthar BN. Impact of ABT based control strategies on ALFC and AVR in DFIG-integrated interconnected power systems. e-Prime-Advances in Electrical Engineering, Electronics and Energy. 2024;9:100665.

[44] Ali T, Malik SA, Hameed IA, Daraz A, Mujlid H, Azar AT. Load frequency control and automatic voltage regulation in a multi-area interconnected power system using nature-inspired computation-based control methodology. Sustainability. 2022;14(19):12162.

[45] Nahas N, Abouheaf M, Darghouth MN, Sharaf A. A multi-objective AVR-LFC optimization scheme for multi-area power systems. Electric Power Systems Research. 2021;200:107467.

[46] Shahgholian G. An overview of hydroelectric power plant: Operation, modeling, and control. Journal of Renewable Energy and Environment. 2020;7(3):14-28.

[47] Babu NR, Chiranjeevi T, Saha A, Bhagat SK. Comparative analysis of various energy storage systems in a conventional LFC system considering RDSTS, PWTS and AHVDC models. Journal of Engineering Research. 2023;11(4):425-36.

[48] Rahman A, Saikia LC, Sinha N. Load frequency control of a hydro-thermal system under deregulated environment using biogeography-based optimised three-degree-of-freedom integral-derivative controller. IET generation, transmission & distribution. 2015;9(15):2284-93.

[49] Grover H, Verma A, Bhatti T. A fast and robust DOBC based frequency and voltage regulation scheme for future power systems with high renewable penetration. Energy Conversion and Economics. 2023;4(4):287-302.

[50] Zhao X, Gong S, Fu B, Gong C. A Time-Varying Hierarchical Load Frequency Control Method for Multi-area Power System with Wind Power Participation and HVDC Tie-Line based on MAS Structure. Journal of Electrical Engineering & Technology. 2023;18(3):1523-37.

[51] Toularoud MS, Rudposhti MK, Bagheri S, Salemi AH. A hierarchical control approach to improve the voltage and frequency stability for hybrid microgrids-based distributed energy resources. Energy Reports. 2023;10:2693-709.

[52] Kunya AB. Hierarchical bi-level load frequency control for multi-area interconnected power systems. International Journal of Electrical Power & Energy Systems. 2024;155:109600.

[53] Gaber ES, MIKHAYLOV A, BARANYAI N, AHMED M, HEMEIDA M. Optimal load frequency control system for two-area connected via AC/DC link using cuckoo search algorithm. Virtual Reality & Intelligent Hardware. 2025;7(3):299-316.

[54] Shan Y, Ma L, Yu X. Hierarchical control and economic optimization of microgrids considering the randomness of power generation and load demand. Energies. 2023;16(14):5503.

[55] Rajbongshi R, Saikia LC. Coordinated performance of interline power flow controller and superconducting magnetic energy storage in combined ALFC and AVR system under deregulated environment. Journal of renewable and sustainable energy. 2018;10(4).

[56] Rajbongshi R, Saikia LC. Combined voltage and frequency control of a multi-area multisource system incorporating dish-Stirling solar thermal and HVDC link. IET Renewable Power Generation. 2018;12(3):323-34.

[57] Mok R, Ahmad MA. Fast and optimal tuning of fractional order PID controller for AVR system based on memorizable-smoothed functional algorithm. Engineering Science and Technology, an International Journal. 2022;35:101264.

[58] Roy TK, Oo AMT. Virtual inertia and damping-based cascaded control approach for enhancing load frequency control in low-inertia multi-area power systems. The Journal of Engineering. 2025;2025(1):e70054.

[59] Kalyan CNS, Goud BS, Reddy CR, Bajaj M, Sharma NK, Alhelou HH, et al. Comparative performance assessment of different energy storage devices in combined LFC and AVR analysis of multi-area power system. Energies. 2022;15(2):629.

[60] Ahmed M, Khamies M, Hassan MH, Domínguez-García JL, Kamel S. A modified controller scheme for frequency stability enhancement of hybrid two-area power grid with renewable energy sources. IET Renewable Power Generation. 2023;17(5):1035-67.

[61] Köse E. Optimal control of AVR system with tree seed algorithm-based PID controller. IEEE access. 2020;8:89457-67.

[62] Ali T, Asad M, Touti E, Graba BB, Aoudia M, Abbas G, et al. Terminal voltage and load frequency control in a real four-area multi-source interconnected power system with nonlinearities via OOBO algorithm. IEEE Access. 2024.

[63] Hakimuddin N, Nasiruddin I, Bhatti TS, Arya Y. Optimal automatic generation control with hydro, thermal, gas, and wind power plants in 2-area interconnected power system. Electric Power Components and Systems. 2020;48(6-7):558-71.

[64] Mesrinejad F, Yaghoubi S, Fani B. Secondary frequency control for improved dynamic performance in interconnected power system. Journal of Simulation and Analysis of Novel Technologies in Mechanical Engineering. 2022;14(4):5-12.